

Elastic Correction of Dead-Reckoning Errors in Map Building

Matteo Golfarelli

Dario Maio

Stefano Rizzi

DEIS, Università di Bologna
Bologna, Italy

Abstract

A major problem in map building is due to the imprecision of sensor measures. In this paper we propose a technique, called elastic correction, for correcting the dead-reckoning errors made during the exploration of an unknown environment by a robot capable of identifying landmarks. Knowledge of the environment being acquired is modelled by a relational graph whose vertices and arcs represent, respectively, landmarks and inter-landmark routes. Elastic correction is based on an analogy between this graph and a mechanical structure: the map is regarded as a truss where each route is an elastic bar and each landmark a node. Errors are corrected as a result of the deformations induced from the forces arising within the structure as inconsistent measures are taken. The uncertainty on odometry is modelled by the elasticity parameters characterizing the structure.

1 Introduction

Most mobile robots need a map of the environment to carry out successfully the navigational tasks assigned to them. Several techniques for environment representation have been devised in the literature, including topological maps [9], symbolic graphs labelled with metric information [2] and analogic descriptions [6]. Though in some applications a detailed map of the environment is given to the robot a priori, map building is still an important issue for all the applications in which the environment is unknown and, in general, in order to have a robot exhibit a fully autonomous behaviour.

The problem of building an accurate map of the environment is strictly related to that of self-positioning. Two positioning techniques are typically used (often together), namely *relative* and *absolute*. Relative positioning is based on odometers which estimate the current position by determining the offset from the initial position. Absolute positioning is based either on an absolute sensor such as a GPS [5] or on the possibility of recognizing landmarks by processing data obtained by

sensors such as sonars, lasers, cameras, etc. [8].

Problems influencing the effectiveness of these techniques in the real world are caused by the imprecision of measurements, which produces metric errors. In particular, odometers typically produce both *systematic* and *non-systematic* errors. The former depend entirely on the mobile platform adopted [4]; the latter are due to undesired interactions between the robot and the environment, such as uneven ground. Systematic errors can be predicted; some are deterministic, some can be modelled by a probabilistic distribution (e.g., the encoder finite resolution causes a normally-distributed error). The latter, which we will call dead-reckoning errors, are inherently associated to every sensor, thus they play a significant role in determining the global error; we may assume that they are distributed normally with null mean. Non-systematic errors cannot be predicted, unless some assumptions on the environment can be made or particular sensors are mounted [3].

Our approach to map building can be applied to correct the dead-reckoning errors made by a robot navigating within an environment where landmarks are present; we do not consider topological errors since we assume that the robot is capable of recognizing a landmark it has already met. The environment is modelled by a relational graph whose vertices and arcs represent, respectively, the landmarks sensed and the inter-landmark routes experienced [10]. While exploring the environment, the robot calculates the relative position of each landmark compared to the one met immediately before, by applying dead-reckoning; when it meets a landmark it has already seen, self-positioning and error correction are achieved together by combining the new measurements collected with the knowledge accumulated so far.

The original contribution of our approach is to found error correction on an analogy between the graph modelling the environment and a mechanical structure: the map is regarded as a truss where each route is an elastic bar and each landmark a node. Errors are corrected as a result of the deformations induced by the forces arising within the structure as inconsistent measurements are taken. The elasticity parameters characterizing the

structure are used to model the uncertainty on odometry.

The main advantage of our approach as compared to those proposed in the literature (e.g. [2] [7] [12]) is that it takes into account all the information previously collected in order to evaluate the correctness of the new measurements being acquired.

2 Uncertainty in Self-Positioning

Let the *pose* of the robot at time step k be expressed by its position in a Cartesian plane, $\mathbf{p}^{(k)} = \begin{bmatrix} x^{(k)} \\ y^{(k)} \end{bmatrix}$, and by its orientation, $\varphi^{(k)}$; the well-known dead-reckoning formula determines the pose at step $k+1$ as a function of the pose at step k and of the moduli of the linear and angular velocities, $w^{(k+1)}$ and $u^{(k+1)}$, respectively, measured by sensors at step $k+1$:

$$\begin{aligned} \mathbf{p}^{(k+1)} &= \begin{bmatrix} x^{(k)} + T w^{(k+1)} \cos\varphi^{(k)} \\ y^{(k)} + T w^{(k+1)} \sin\varphi^{(k)} \end{bmatrix}, \\ \varphi^{(k+1)} &= \varphi^{(k)} + T u^{(k+1)} \end{aligned}$$

where T is the sampling interval of sensors (see Figure 1).

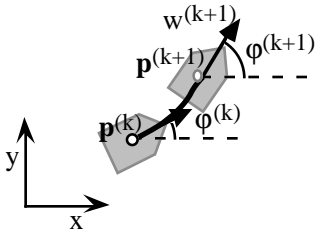


Figure 1. The robot at steps k and $k+1$.

Using this formula, the errors made in measuring the angular velocity $u^{(k+1)}$ accumulate through all the subsequent evaluations of the pose. On the other hand, if the robot mounts a compass, while the new coordinates $x^{(k+1)}$ and $y^{(k+1)}$ are still calculated as above, $\varphi^{(k+1)}$ may be measured directly; thus, each new positional estimate is not affected by the errors made in measuring the robot's orientation at the previous steps.

In [15] an estimate of the positional uncertainty for a robot moving along a path and calculating its current position by odometers is derived. Each position calculated is associated with a density function expressing the probability that, due to errors in measurements, the robot is positioned in the surrounding area:

$$\begin{aligned} \delta(x,y, \mathbf{C}^{(k)}) &= \frac{1}{2\pi |\mathbf{C}^{(k)}|^{1/2}} \cdot \\ &\cdot \exp\left(-\frac{1}{2} \begin{bmatrix} x - x^{(k)} \\ y - y^{(k)} \end{bmatrix} (\mathbf{C}^{(k)})^{-1} \begin{bmatrix} x - x^{(k)} & y - y^{(k)} \end{bmatrix}\right) \end{aligned}$$

The area in which the robot may stand with non-

negligible probability is an ellipse whose shape and dimensions depend on the length and complexity of the path, and is represented by the covariance matrix $\mathbf{C}^{(k)}$ [1]. Similarly, an estimate of the probability density function of the position for a robot mounting a compass can be derived.

3 Elastic Correction

The map built by the robot is structured as a non-directed graph $\mathcal{M}=(V,R)$. Each vertex $v_i \in V$ represents a landmark sensed and is labelled with its estimated position $\mathbf{p}_i = \begin{bmatrix} x_i \\ y_i \end{bmatrix}$; arc $r_{ij} \in R$ represents the route connecting v_i and v_j and is labelled with the number of times the route has been covered so far, t_{ij} . We will denote by ϑ_{ij} (*route orientation*, $0 \leq \vartheta_{ij} < \pi$) the absolute orientation of the segment connecting v_i to v_j , and by s_{ij} (*route stretch*) its length, calculated as the Euclidean distance between \mathbf{p}_i and \mathbf{p}_j . Every time the robot moves from v_i to v_j covering the corresponding route, the covariance matrix expressing the uncertainty induced on the position of v_j is calculated; the value of the covariance matrix depends on the length and on the tortuosity of the route covered. Arc r_{ij} is labelled with the average of the t_{ij} covariance matrices calculated, \mathbf{C}_{ij} .

Error correction may be framed within the exploration algorithm as follows:

```

L = ();
/* list of the routes on which first-sight
/* correction must be applied
do
  reach landmark v_j by covering route r_ij;
  if r_ij never covered before
  { if v_j never met before
    add r_ij to L;
    else
    { apply first-sight correction to L' ⊆ L;
      L = L - L';
    }
  }
  else
  apply refinement correction to r_ij;
loop

```

It is remarkable that our correction technique works independently of the specific sensors used for dead-reckoning: in fact, it can be used by a robot mounting a compass as well as by a robot using only odometers. Of course, since in the first case the robot's positional uncertainty is lower, the residual error after correction will be significantly smaller.

3.1 Environment modelling

Elastic correction is based on the analogy between the environment map \mathcal{M} and a pin-jointed truss whose elements and nodes represent, respectively, routes and landmarks (see Figure 2); the parameters defining the stiffness of each element when loaded sum up the characteristics of the corresponding route. The more elastic an element, the greater the change in length and orientation that it will experience when loaded; thus, stiffness should be proportional to the certainty on the stretch and orientation of the corresponding route.

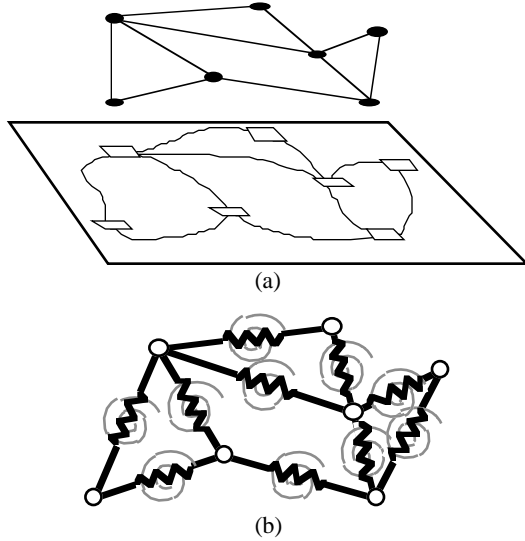


Figure 2. Graph-based representation of an environment (a) and equivalent truss (b).

An element representing a route r with stretch s and orientation ϑ may be thought of as a bar long s , oriented according to ϑ and behaving as follows:

- it can be compressed elastically along its axis to model uncertainty on the route stretch, s ;
- it can neither be bended nor twisted;
- it can rotate elastically to model uncertainty on the route orientation, ϑ .

From a mechanical point of view, a bar with these characteristics can be modelled by combining a linear axial spring and a rotational spring (see Figure 3), whose spring constants k_a and k_r must be defined in function of the probability density function of the robot position.

For simplicity, we consider a bar representing a route r oriented along the x axis ($\vartheta=0$). Since k_a expresses an axial deformation along x , it is reasonable to define it in terms of the average error Δx made by the robot in determining the x coordinate of the other end of r , i.e., the average error made on the stretch of r :

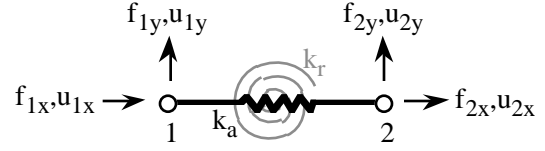


Figure 3. Truss basic element, including a linear elastic spring (in black) and a rotational elastic spring (in grey).

$$k_a \propto \frac{1}{\Delta x},$$

where

$$\Delta x = \int_{-\infty}^{+\infty} \int_{-\infty}^{+\infty} \delta(x,y,\mathbf{C}) |x| dx dy = \sqrt{\frac{2}{\pi} C_{11}}$$

and \mathbf{C} is the covariance matrix for r .

Similarly, it is possible to calculate the average error Δy made by the robot in determining the y coordinate of the other end of r . Since k_r does not express an axial deformation along y , it is necessary to determine the spring constant k_r' of a linear spring which, under certain conditions, may be equivalent to the rotational one. It turns out to be

$$k_r = s^2 k_r'$$

Thus we may assume

$$k_r \propto \frac{s^2}{\Delta y},$$

where

$$\Delta y = \int_{-\infty}^{+\infty} \int_{-\infty}^{+\infty} \delta(x,y,\mathbf{C}) |y| dx dy = \sqrt{\frac{2}{\pi} C_{22}}$$

The certainty on the stretch and orientation of route r also depends on the number t of times r has been covered; in fact, the higher t , the higher the amount of data concerning r collected. The *stiffness matrix* for a bar representing a route r oriented along the x axis turns out to be

$$\mathbf{K} = \begin{bmatrix} \frac{t}{\Delta x} & 0 & -\frac{t}{\Delta x} & 0 \\ 0 & \frac{t}{\Delta y} & 0 & -\frac{t}{\Delta y} \\ -\frac{t}{\Delta x} & 0 & \frac{t}{\Delta x} & 0 \\ 0 & -\frac{t}{\Delta y} & 0 & \frac{t}{\Delta y} \end{bmatrix}$$

The stiffness matrix for a bar representing a route r oriented along direction ϑ is obtained by

1. rotating by $-\vartheta$ the covariance matrix \mathbf{C} ;
2. calculating Δx and Δy by formulae;

3. building the stiffness matrix \mathbf{K} ;
4. rotating \mathbf{K} by ϑ .

The stiffness matrix for the whole structure is assembled by superimposing the stiffness matrices of the single elements belonging to the structure. The displacements of the nodes can then be solved by applying the *stiffness method* [11].

3.2 Correction of first-sight errors

Suppose the robot is exploring an unknown area starting from a known landmark v_0 . It meets the unknown landmarks v_1, \dots, v_{m-1} by covering a sequence of unknown routes, and finally reaches a landmark v_m which it has already met either before or during the current exploration session. If v_m has been met before v_0 , the segments orderly connecting v_0 to v_m form an open polygonal (see Figure 4.a). Otherwise, let $0 \leq k < m-1$ such that $v_k \equiv v_m$; in this case, the segments orderly connecting v_k to v_m form a closed polygonal (see Figure 4.b). When v_m is reached, the new positional estimate \mathbf{p}''_m computed by dead-reckoning may be compared to the previous one, \mathbf{p}'_m ; due to sensor errors, the two estimates will almost certainly differ. Let

$$\bar{\mathbf{u}}_m = \mathbf{p}''_m - \mathbf{p}'_m$$

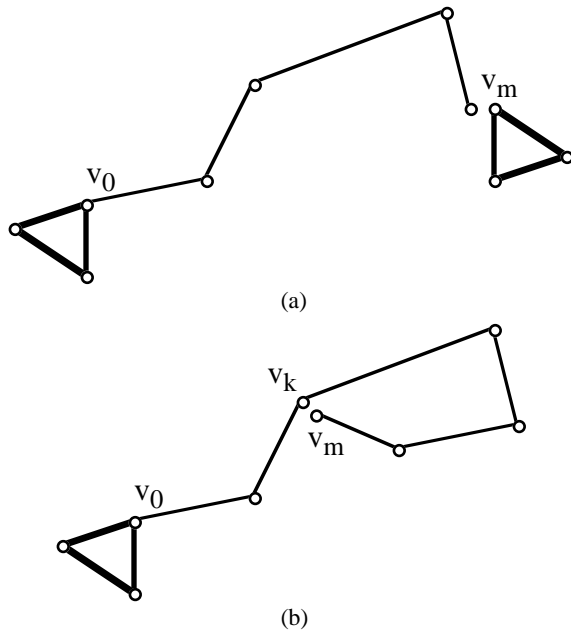


Figure 4. Error correction on open (a) and closed (b) polygonals.

The graph representing the environment should be metrically consistent at each time during exploration, hence, the two positional estimates for v_m must be forced

to agree exactly. We assume the error on the stretch of each route to be proportional to the positional uncertainty induced by that route. On our mechanical model, this corresponds to

- constraining v_0 and applying a displacement $\bar{\mathbf{u}}_m$ to v_m if the polygonal is open;
- constraining v_k and applying a displacement $\bar{\mathbf{u}}_m$ to v_m if the polygonal is closed.

In both cases, the displacement applied moves v_m in position \mathbf{p}'_m thus restoring the metric consistency of the graph; the displacements calculated for the free nodes determine the new positions for the landmarks involved.

Figure 5 shows an example for a simple closed polygonal.

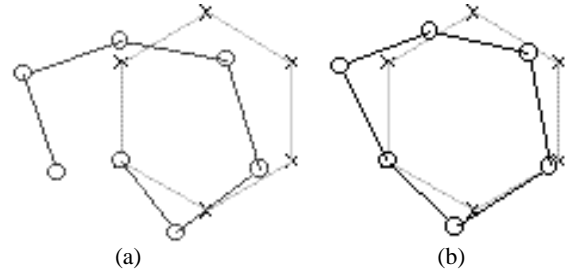


Figure 5. Elastic correction on a regular hexagon. The real graph is in light grey; the measured one in dark grey (a); the corrected one is in black (b).

3.3 Refinement of map measurements

Every time the robot covers a route r_{ij} it has covered before, it can exploit the new information acquired to improve the current estimate of the stretch and orientation of r_{ij} and, thus, that of the positions of its end landmark v_i and v_j . Reasonably, the estimates for r_{ij} should be equal, at each time, to the average of the data measured so far. The desired displacements for v_i and v_j are calculated by imaging to rotate r_{ij} around its midpoint in order to let it assume the new stretch and orientation.

This solution is not satisfactory since it does not take into account all the knowledge of the environment collected so far, while using global knowledge to correct the error on a single route is essential when the certainty on the routes is not evenly distributed. Another issue arising when correcting the error on a route is how metric consistency for the graph representing the environment is maintained: in fact, correcting the stretch and orientation of r_{ij} implies modifying the stretches and orientations of the adjacent routes.

Our mechanical model allows both issues to be addressed. Let \mathcal{M} be the graph representing the

environment, and $r_{ij} \in \mathcal{M}$ be the last route experienced. Our approach consists of two phases:

1. The forces $\bar{\mathbf{f}}_i$ and $\bar{\mathbf{f}}_j$ producing the desired displacements $\bar{\mathbf{u}}_i$ and $\bar{\mathbf{u}}_j$ on the ends of r_{ij} are calculated on a reference structure including r_{ij} and the two adjacent routes of maximum stiffness, r_{ih} and r_{jk} ; both r_{ih} and r_{jk} are constrained in the vertices not shared with r_{ij} (see Figure 6).

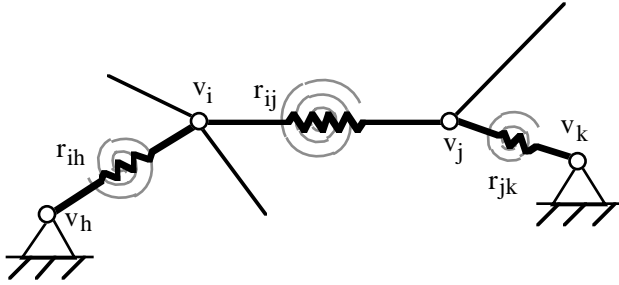


Figure 6. Reference structure for calculating the forces to be applied.

2. The forces calculated in the previous phase for v_i and v_j , $\bar{\mathbf{f}}_i$ and $\bar{\mathbf{f}}_j$, are applied to v_i and v_j within a larger structure including the set of routes connecting the η landmarks nearest to r_{ij} .

It should be noted that choosing a value η for the number of free nodes in the structure entails determining an upper bound on the computational complexity of each correction. Conversely, the lower η is, the less effective error correction is. Thus, the design of η may be guided by two different criteria:

- If limiting computational complexity is a relevant issue for the current application, a proper value should be fixed and maintained during navigation (in most of our tests we used $\eta=50$).
- Otherwise, η should be estimated before each correction, based on the magnitude of the force applied and on the pattern of connectivity of the map, as the number of nodes $\bar{\eta}$ which are expected to undergo a non negligible displacement.

Simulations showed that, by reducing η up to 25%, the average error on the route lengths does not increase significantly (less than 10%).

4 Experimental Results

The robot platform on which we are experimenting our approach is a Pioneer I (by Real World Interface); it mounts a sonar array and a camera for obstacle avoidance

and landmark identification, as well as a fluxgate compass and a pair of wheel encoders to determine its position. We have extensively tested the elastic correction technique on a set of environments in order to evaluate its effectiveness and robustness. The tests presented in this section are based on the sensorial model of the Pioneer I robot. In particular, the sensory covariance matrix was measured by means of a set of experiments carried out on the robot; the (absolute) average odometric and compass errors turned out to be, respectively, 5% of the distance measured and 0.03 radians.

We estimate the error on the map metric by two measurements: the average percentage error on the stretch of the routes, σ , and the average error on the orientation of the routes, ρ .

Some tests focus on comparing our approach with one which estimates the stretch and orientation of each route as the weighted average of the measurements acquired so far for that route. Please note that the weighted average technique does not constrain the extremes of pairs of adjacent routes to overlap; thus, it does not guarantee the metric consistency of the map. Nevertheless, we believe this comparison is useful to prove that using global besides local knowledge leads to more effective corrections of the metric errors. The other correction methods proposed in the literature can hardly be quantitatively compared with elastical correction, since they are either based on assumptions and sensory equipments radically different from ours [7] [13] or were devised within a different framework [14].

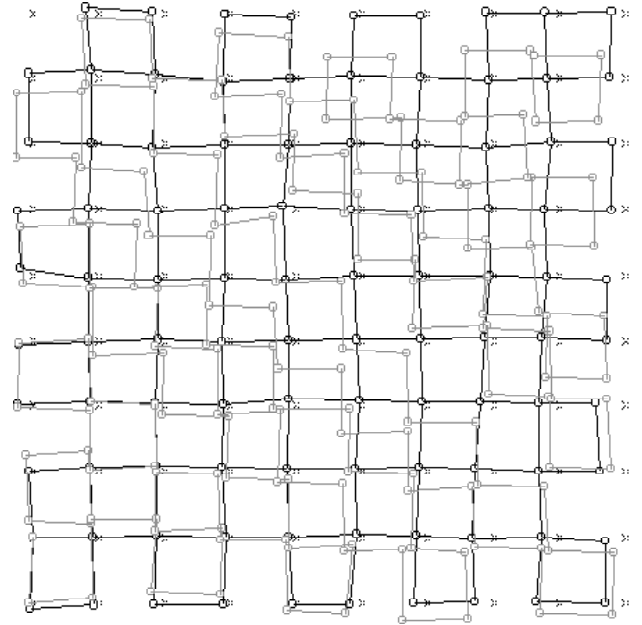


Figure 7. First-sight correction. The measured map is grey, the corrected one is black; crosses represent the true positions of vertices.

Figure 7 and Table I show the result of first-sight correction on a square-meshed map. This phase is primarily aimed at eliminating the metric inconsistencies due to sensor errors; the resulting map is consistent but still affected by a significant error.

	σ	ρ
before correction	0.049	0.033
after correction	0.046	0.032

Table I. Errors for the first-sight correction in Figure 7.

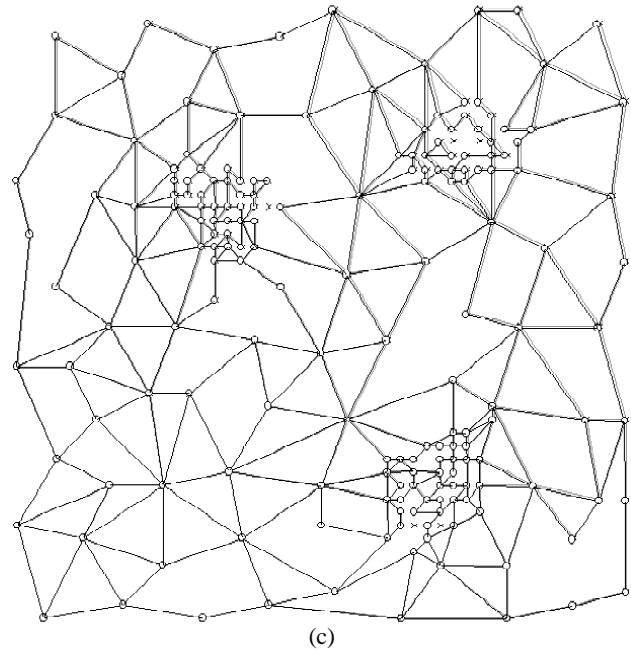
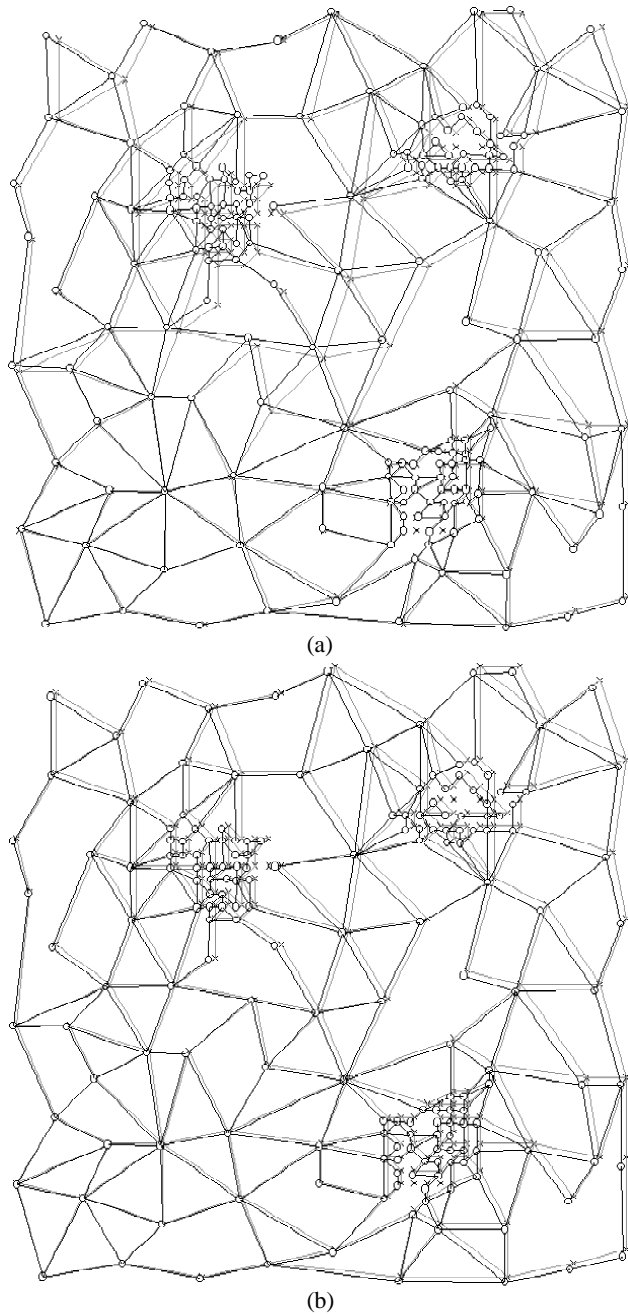


Figure 8. Correction after 1 tour (a), after 5 tours (b), after 50 tours (c). The true maps are grey, the corrected ones are black.

Figures 8 and 9 show the result of refinement correction on a map being toured several times; it is remarkable that both errors are already reduced by half after 3 complete tours of the map. Both error measurements adopted are referred to routes, that is, to the relative positioning of landmarks, which we believe to be the most relevant issue from the point of view of planning and executing navigational tasks. Nevertheless, we have also considered the absolute positioning of landmarks; it turned out that the average error on the landmark positions reduced to 20÷30% of the one measured before correction during the first 10 tours and dropped below 10% in the following tours.

We have carried out some tests assuming that the odometric and compass errors were higher than those measured on the Pioneer I: 8% and 0.08 radians, respectively. The errors on stretch and orientation are still reduced by half after 3÷4 tours of the map.

We have also carried out some experiments aimed at determining the behaviour of our technique when the average odometric and compass errors are strongly unbalanced. The results confirm that both errors are reduced by half after 3÷4 tours. These tests prove that the effectiveness of our approach does not depend on the amount of sensory errors and confirm that the mathematical model adopted distributes corrections properly on the map.

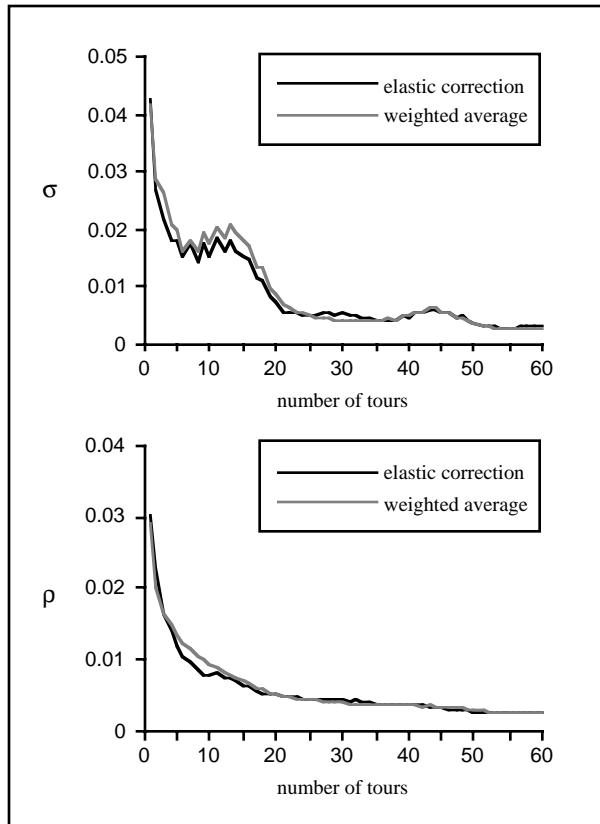


Figure 9. Comparison between elastic correction and weighted average for the map in Figure 8.

5 Conclusion

In this paper we have presented a technique for correcting sensory errors during a map building process in mobile robots; error correction is based on an analogy between the graph modelling the environment and a mechanical structure whose elasticity parameters model the uncertainty on odometry. The experimental tests confirm the effectiveness of our technique in reducing the global metric error and prove its robustness with reference to the amount of error.

References

- [1] M. Adams *et al.*, "Control and localisation of a post distributing mobile robot," in *Int. Conf on Intelligent Robots and System*, Munich, 1994, pp. 150-156.
- [2] K. Basye, T. Dean and J.S. Vitter, "Coping with uncertainty in map learning," in *Proc. 11th Int. Joint Conf. on Artificial Intelligence*, 1989, pp. 347-352.
- [3] J. Borenstein, "The CLAPPER: a dual-drive mobile robot with internal correction of dead-reckoning errors," in *Proc. IEEE Int. Conf. on Robotics and Automation*, San Diego, CA, 1994, pp. 3085-3090.
- [4] J. Borenstein and L. Feng, "Measurement and correction of systematic odometry errors in mobile robots," *IEEE Trans. On Robotics and Automation*, vol. 12, no. 6, 1996.
- [5] S. Cooper and H. Durrant-Whyte, "A Kalman filter for GPS navigation of land vehicles," in *Proc. Int. Conf on Intelligent Robots and System*, Munich, 1994, pp. 157-163.
- [6] A. Elfes, "Sonar-based real-world mapping and navigation," *IEEE Journ. of Robotics and Automation*, vol. 3, no. 3, pp. 249-265, 1987.
- [7] S.P. Engelson and D. V. McDermott, "Error correction in mobile robot map learning," in *Proc. IEEE Int. Conf. On Robotics and Automation*, 1992.
- [8] M. Golfarelli, D. Maio and S. Rizzi, "A hierarchical approach to sonar-based landmark detection in mobile robots," in *Proc. 5th Symp. on Intelligent Robotics Syst.*, Stockholm, Sweden, 1997, pp. 77-84.
- [9] D. Kortenkamp and T. Weymouth, "Topological mapping for mobile robots using a combination of sonar and vision sensing," in *Proc. AAAI'94*, 1994.
- [10] D. Maio, D. Maltoni and S. Rizzi, "Dynamic Clustering Of Maps In Autonomous Agents," *IEEE Trans. Pattern Analysis and Machine Intelligence*, vol. 18, no. 11, pp. 1080-1091, 1996.
- [11] H.C. Martin, *Introduction to matrix methods of structural analysis*, McGraw-Hill, 1966.
- [12] M. Mataric, "A distributed model for mobile robot environment-learning and navigation," *Technical Report 1228*, MIT Artificial Intelligence Lab., 1990.
- [13] H. Shatkay and L.P. Kaelbling, "Learning topological maps with weak local odometric information," in *Proc. 15th Int. Joint Conf. on Artificial Intelligence*, Nagoya, 1997, pp. 920-927.
- [14] H. Sugiyama, "A method for an autonomous mobile robot to recognize its position in the global coordinate system when building a map," in *Proc. 1993 IEEE/RSJ Int. Conf. on Intelligent Robotics and Systems*, Yokohama, 1993, pp. 2186-2191.
- [15] Y. Tonouchi, T. Tsubouchi and S. Arimoto, "Fusion of dead-reckoned positions with a workspace model for a mobile robot by bayesian inference," in *Proc. Int. Conf. on Intelligent Robots and System*, Munich, 1994, pp. 1347-1354.